European Journal of Radiology 115 (2019) 66–73

Contents lists available at ScienceDirect

European Journal of Radiology

journal homepage: www.elsevier.com/locate/ejrad

Research article

Prognostic value of preoperative dynamic contrast-enhanced magnetic resonance imaging in epithelial ovarian cancer☆

Auni Lindgren[a,*], Maarit Anttila[a,b], Otso Arponen[c], Suvi Rautiainen[c], Mervi Könönen[c,d], Ritva Vanninen[c,e,f], Hanna Sallinen[b]

[a] University of Eastern Finland, Faculty of Health Sciences, School of Medicine, Institute of Clinical Medicine, Obstetrics and Gynecology, Finland
[b] Department of Gynecology, Kuopio University Hospital, Kuopio, Finland
[c] Department of Clinical Radiology, Kuopio University Hospital, Kuopio, Finland
[d] Department of Clinical Neurophysiology, Kuopio University Hospital, Kuopio, Finland
[e] University of Eastern Finland, Faculty of Health Sciences, School of Medicine, Institute of Clinical Medicine, Clinical Radiology, Finland
[f] University of Eastern Finland, Cancer Center of Eastern Finland, University of Eastern Finland, Kuopio, Finland

ARTICLE INFO

Keywords:
Ovarian cancer
Magnetic resonance imaging
Dynamic contrast-enhanced imaging
Biomarkers
Prognosis

ABSTRACT

Objectives: To investigate whether semi-quantitative and pharmacokinetic perfusion dynamic contrast-enhanced (DCE) parameters are associated with traditional prognostic factors and can predict clinical outcome in ovarian cancer (OC).

Methods: This prospective study, approved by local ethical committee, enrolled 38 patients with primary OC, 2011–2014. After preoperative DCE-MRI (3.0 T), two observers measured perfusion (K^{trans}, K_{ep}, V_e, V_p) and semi-quantitative parameters (area under the curve, peak, time-to-peak) by drawing regions of interest (ROIs) covering the large solid lesion (L-ROI) and the most enhancing small area (S-ROI) (NordicICE platform). Kruskal–Wallis was used to analyze associations between MRI parameters and classified prognostic factors.

Results: Mean K^{trans} values were higher in high-grade serous OC than in other types (L-ROI, P = 0.041; S-ROI, P = 0.018), and lower mean K^{trans} values predicted residual tumor (L-ROI P = 0.030; S-ROI, P = 0.012). Higher minimum V_p values were associated with higher International Federation of Gynecology and Obstetrics (FIGO) stage (S-ROI, P = 0.023).Shorter recurrence-free survival was predicted by higher V_e (minimum L-ROI, P = 0.035; maximum S-ROI, P = 0.046), V_p (maximum S-ROI, P = 0.033), and lower time-to-peak (maximum S-ROI, P = 0.047) in Kaplan–Meier analysis. Multiparametric MRI variables combining DCE and diffusion weighted data were also predictive for survival.

Conclusion: DCE-MRI parameters may represent imaging biomarkers for predicting tumor aggressiveness and prognosis in OC. Higher K^{trans} levels were associated with better results in cytoreductive surgery but with earlier recurrence.

1. Introduction

Ovarian cancer (OC) is the fifth most common cancer and fourth most common cause of cancer mortality in women [1]. Characterizing ovarian masses as precisely as possible is important because treatment modalities are tailored individually, and especially during a woman's reproductive years, conservative surgery for fertility-sparing can be crucial. Vaginal ultrasonography is the initial modality for investigating ovarian tumors, and the International Ovarian Tumor Analysis group guideline can be used to estimate the malignancy risks of ovarian tumors [2]. Approximately 20% of ovarian tumors remain indeterminate after an ultrasound conducted by a specialist. Also the risk of

Abbreviations: EES, extravascular, extracellular space; K^{trans}, a rate constant for transfer of contrast agent from plasma to EES; K_{ep}, rate constant for transfer of contrast agent from EES to plasma; V_e, contrast agent distribution volume, EES volume fraction; V_p, plasma volume fraction; AUC, area under the enhancement curve; WashIn, initial up-slope of the DCE curve; WashOut, initialdown-slope of the DCE curve; Peak, peak/maximal enhancement; Time To Peak, time when contrast agent reaches the peak volume; AIF, arterial input function; NACT, neoadjuvant chemotherapy; mpMRI, multiparametric MRI

☆ Work originated: Kuopio University Hospital, P.O. Box 100, Kuopio.

* Corresponding author at: Department of Gynecology and Obstetrics, Kuopio University Hospital, P.O. Box 100, Kuopio, FIN-70029, KYS, Finland.
E-mail addresses: Auni.lehikoinen@gmail.com (A. Lindgren), maarit.anttila@kuh.fi (M. Anttila), otso.arponen@kuh.fi (O. Arponen), suvi.rautiainen@icloud.com (S. Rautiainen), mervi.kononen@kuh.fi (M. Könönen), ritva.vanninen@kuh.fi (R. Vanninen), hanna.sallinen@kuh.fi (H. Sallinen).

https://doi.org/10.1016/j.ejrad.2019.03.023
Received 4 January 2019; Received in revised form 20 March 2019; Accepted 29 March 2019

malignancy index (RMI) helps physicians differentiate benign from malignant lesions [3]. Magnetic resonance imaging (MRI) is valuable especially in diagnostics of this indeterminate group in US and intermediate- and low-risk ovarian tumors (RMI < 200), giving better soft tissue contrast than computed tomography (CT). Also in ovarian cancer diagnostics MRI can yield more robust information than CT. Diffusion weighted imaging (DWI) has shown promise in tumor staging, predicting the aggressiveness of tumor and clinical outcome [4,5]. Cancer treatment is becoming individualised, so it is important to further study the possibilities to obtain more information also in diagnostic imaging. If it was possible to identify patients who can be operated optimally in sytoreductive surgery and define the patient group with most aggressive tumors with preoperative imaging, it could be very valuable in the decision-making of treatment options.

Dynamic contrast-enhanced (DCE) MRI is used to improve the diagnostic accuracy of conventional MRI, with proven importance in differential diagnostics and preoperative evaluation for breast, prostate, and kidney tumors, among others [6–8]. DCE-MRI can distinguish malignant from benign tumors based on differences in contrast agent behavior; in malignant tumors, the microcirculation is different because of neoangiogenesis [9,10]. Most DCE-MRI studies of ovarian tumors have targeted differentiating among benign, borderline, and malignant tumors [11–14], and studies often have used semi-quantitative and time intensity curve–based parameters [11–13]. European Society of Urogenital Radiology guidelines advocate inclusion of DCE time intensity curve analysis to specify indeterminate ovarian masses [15].

Because the volume of transfer constant (K^{trans}) level is influenced by blood flow and vessel permeability properties, it has been under active investigation to be used as a biomarker of tumor perfusion and permeability in DCE-MRI cancer studies [16–21], with contradictory results. Also other pharmacokinetic perfusion parameters reflect the physiology of circulation in the microvasculature and can be quantitatively compared among different patients and investigators [9,22]. Therefore, DCE imaging might provide more extensive prognostic information in OC, as well.

We hypothesized that DCE parameters will differ between highly aggressive OC and less severe disease. The main objectives of the present study were to investigate whether semi-quantitative and perfusion DCE parameters are associated with traditional prognostic factors and able to predict the clinical course of OC. Our secondary objectives were to investigate the possible inter-technique differences related to ROI size and analyze interobserver variability in DCE measurements.

2. Materials and methods

2.1. Study protocol and patients

This exploratory prospective single-institution study was conducted between January 2011 and December 2014. The local research ethical committee approved the study protocol, and written informed consent was obtained. The inclusion criteria were a clinical diagnosis of primary OC, fallopian tube cancer, or peritoneal carcinoma and measurable disease at staging CT. Exclusion criteria were contraindications to MRI or gadolinium contrast agents. A total of 38 patients were enrolled. These patients were used also in our previous article concentrating on ADC values [5]. In the current study we have analysed the possible predictive value of the DCE parameters, both alone and combined with ADC values, now with an extended follow-up in survival analysis. Cancers were staged using the International Federation of Gynecology and Obstetrics (FIGO) guidelines. Histological type and grade were evaluated according to World Health Organization criteria. First-line treatment was chosen by an experienced multidisciplinary team (surgery, n = 34; neoadjuvant chemotherapy (NACT) before surgery, n = 4). Patients received paclitaxel–carboplatin as adjuvant chemotherapy after the operation, excluding a patient with stage 1A disease who received carboplatin monotherapy. Patient characteristics are described in Table 1.

Table 1
Clinicopathological characteristics of patients with ovarian cancer (n = 35).

Variable	n (%) /median[range]
Age years	67 [47-86]
BMI	26 [17.4-40]
CA-125	483 [16-5234]
Stage at diagnosis	
I	5 (14.3)
II	2 (5.7)
III	14 (40)
IV	14 (40)
Histological type	
Serous high grade	23 (65.7)
Endometrioid	5 (14.3)
Mucinous	1 (2.9)
Clear cell	1 (2.9)
Other	5 (14.3)
Stage in high grade serous	other
I	2 (8.7) 3 (25.0)
II	1 (4.3) 1 (8.3)
III	9 (39.1) 5 (41.7)
IV	11 (47.8) 4 (25.0)
Primary residual tumor a	
None	16 (47.1)
≤ 1 cm	14 (41.2)
> 1 cm	4 (11.8)
Chemotherapy response b	
Complete response	25 (71.4)
Partial response	2 (5.7)
Stable disease	0
Progressive disease	8 (22.9)
Tumor recurrence c	
No recurrence	11 (40.7)
Recurrence	16 (59.3)
Platinum sensitivity	
Sensitive	25 (71.4)
Resistant	10 (28.6)
Patient status	
Dead, ovarian cancer	21 (60)
Alive	14 (40)

BMI = body mass index, [a] one patient did not enter to surgery because of overall situation, [b] four patient who received neoadjuvant chemotherapy and 3 dose of adjuvant chemotherapy after surgery are also included to final chemotherapy response analysis, [c] patients with progressive disease were not included to recurrence estimation.

2.2. Imaging protocol

All patients underwent 3.0 T MR imaging (Philips Achieva 3.0 T TX, Philips N.V., Eindhoven, The Netherlands) before treatments. The MRI protocol included T2w, T1w (non-contrast and contrast enhanced), diffusion-weighted imaging (DWI) and DCE sequences for dynamic analysis (Table 2). During DCE image acquisition, non-contrast images were scanned first (image stack 1), followed by contrast agent administration, and continued image acquisition (image stacks 2–23). The contrast agent gadoterate meglumine (Dotarem® 279.3 mg/ml, Guerbet, France) was injected intravenously as a bolus dose of 0.1 mmol/kg at a rate of 4 ml/s, followed by a 20 ml flush of 0.9% sodium chloride solution using an MRI-compatible power injector (Optistar Elite, Covidien, Los Angeles, CA, USA). T1w postcontrast images were scanned 3D.

2.3. Image analysis

Structural MR images were evaluated independently and blinded to histological information by two observers (AL, OA), with 4 and 3 years of experience in MRI, using a Sectra PACS workstation (IDS7, Version 15.1.20.2, Sectra AB, Linköping, Sweden). A senior radiologist (SR)

Table 2
Imaging protocol.

Sequence acquisition time	Orientation	TR (ms)	TE (ms)	Flip angle (°)	FatSat	Resolution (mm)	N slices (gap mm)	SENSE factor	Other
T2W_TSE *0:41.3*	tra	Shortest	80	90	–	0.7 × 0.7 × 5.0	52 (0.5)	2.0	Breath hold
T2W_TSE *0:35.9*	sag	Shortest	80	90	–	0.7 × 0.7 × 5.0	61 (0.5)	2.0	Breath hold
T2W_TSE *0:33.0*	cor	Shortest	80	90	–	0.7 × 0.7 × 5.0	58 (0.5)	2.0	Breath hold
DWIBS *3:35.7*	tra	Shortest	Shortest	–	–	1.3 × 1.3 × 5.0	62 (0)	2.0	b = 800
DWI_3b *3:40.6*	tra	Shortest	Shortest	–	STIR	1.8 × 1.8 × 5.0	56 (0.5)	2.0	b = 0, 300, 600
dual_FFE *1:13.4*	tra	180	1.15 (outphase) 2.30 (inphase)	55	–	1.3 × 1.3 × 5.0	56 (0.4)	2.0	Breath hold
Dyn_eTHRIVE 2:38	tra	Shortest	Shortest	10	SPAIR	0.9 × 0.9 × 5.0	51 (0)	2.3	Dyn scan time 6.7 sec
T1_FS_3D 0:20.2	tra	Shortest	Shortest	10	SPAIR	1.5 × 1.5 × 3.0	147 (-1.5)	2.0	Breath hold

TR = repetition time, TE = echo time, FatSat = fat saturation, N slices = number of slices, tra = transversal, sag = sagittal, cor = coronal, TSE = turbo spin echo, DWIBS = diffusion-weighted imaging with background body signal suppression, STIR = short tau inversion recovery, SPAIR = spectral attenuated inversion recover, FFE = fast field echo, Dyn_eTHIRIVE = Dynamic contrast-enhanced T1 high-resolution isotropic volumetric examination.

with 11 years of experience verified the identification and delineation of ADC measurements.

DCE-MRI parameter maps were generated automatically using NordicICE (version: 2.3.13, NordicNeuroLab, Bergen, Norway). Motion correction was done automatically. Five semi-quantitative parameter maps were generated from the DCE curve: area under the DCE curve; WashIn, the initial up-slope of the DCE curve; WashOut, down-slope of the DCE curve; peak, the amplitude of peak enhancement; and time-to-peak, the time when contrast agent reaches peak enhancement. To quantitate the perfusion the arterial input function was determined by using a small AIF ROI from the common or external iliac artery. Four quantitative parameter maps were generated: K^{trans}, a rate constant for transfer of contrast agent from plasma to the extravascular extracellular space (EES); K_{ep}, the rate constant from EES to plasma; V_e, contrast agent distribution volume (% volume of EES per unit volume of tissue); V_p, plasma volume. Measurements were obtained using the transaxial image showing the largest solid tumor diameter in the ovary. In clinical practice two-dimensional measurement is practical and previous evidence from DW imaging supports its use [23].Two different regions of interest (ROIs) were defined: large ROI (L-ROI) was drawn free-hand to cover the whole solid tumor area, excluding necrotic, cystic, and vascular areas; small ROI (S-ROI), circle with a diameter of 6–12 mm, was placed on the area considered most solid and high enhancement identified by visual assessment. T2w, T1w, DWI, and contrast-enhanced T1w sequences were all available for ROI localization and tumor demarcation (Fig. 1). DWI helped to identify the most solid part while the early enhancement time point, the wash in phase, was used for assessment of enhancement. ROIs were drawn on enhancement DCE images and replicated to DCE parameter maps (Fig. 2). Due to the exploratory nature of this study, we selected these potential predictive DCE factors associated with outcome in ovarian cancer from a literature review of oncological MRI. Because of tumor biology complexity and scanty experience with DCE perfusion parameters in OC, mean, maximum, and minimum values were registered from each DCE parameter for analyses. Furthermore, apparent diffusion coefficient (ADC) map was automatically generated from b-values of 0, 300, and 600 mm^2/s. For ADC analysis, the same slice position and ROI placement were used as for the DCE analysis.

2.4. Statistical analysis

SPSS for Windows (Version 22.0, 2013, SPSS Inc., Chicago, IL, USA) was used for statistical analysis. Values are presented as mean ± SD unless otherwise stated. Interclass correlation coefficient (ICC) was used to test interobserver correlation, and the Bland–Altman method was applied to visualize interobserver variability. Kruskal–Wallis and Mann–Whitney U tests were used for classified parameters when appropriate, as were Spearman's test for bivariate correlations for continuous variables, because of non- normal distribution of data. For the survival analyses, DCE parameters were dichotomized using the median as a cut-off. Recurrence-free survival (RFS) was defined as the interval between the date of surgery and the date of identified recurrence, and overall survival (OS) as the interval between the date of surgery and the date of death or the end of follow-up. The Kaplan–Meier method (log-rank) was used for univariate survival analyses, and significant variables from univariate analyses were entered in a stepwise manner for

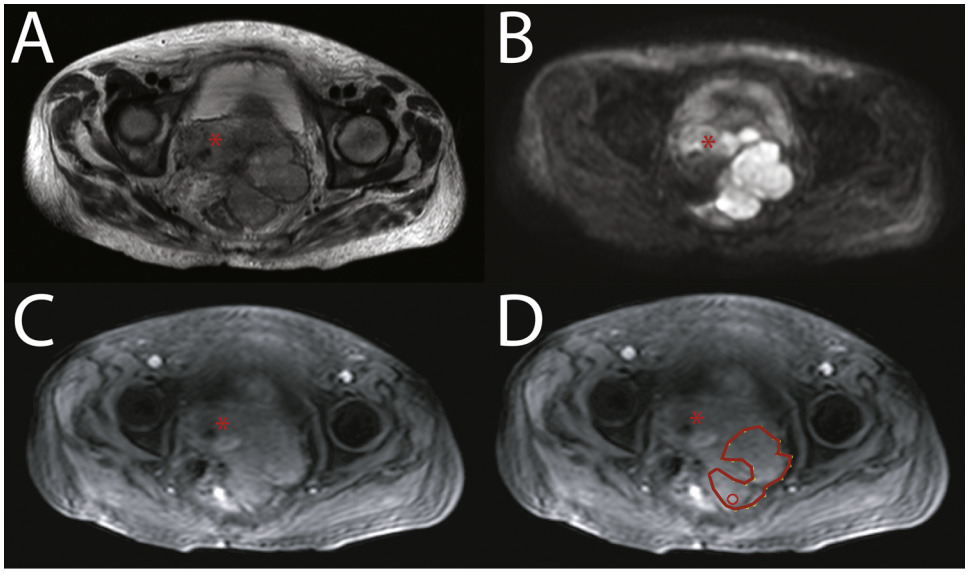

Fig. 1. Images from a 67-year-old woman with high-grade serous ovarian adenocarcinoma. A large pelvic primary tumor is seen on T2-weighted (A), diffusion-weighted (DWIBS, b 800) (B) and dynamic contrast enhancement (C, D) images. A large region of interest (L-ROI) is drawn to cover the whole tumor, excluding the necrotic area in the middle, and a small ROI (S-ROI) is placed on a subregion appearing to be the most enhancing part of the tumor (D). The uterus has been marked with an asterisk.

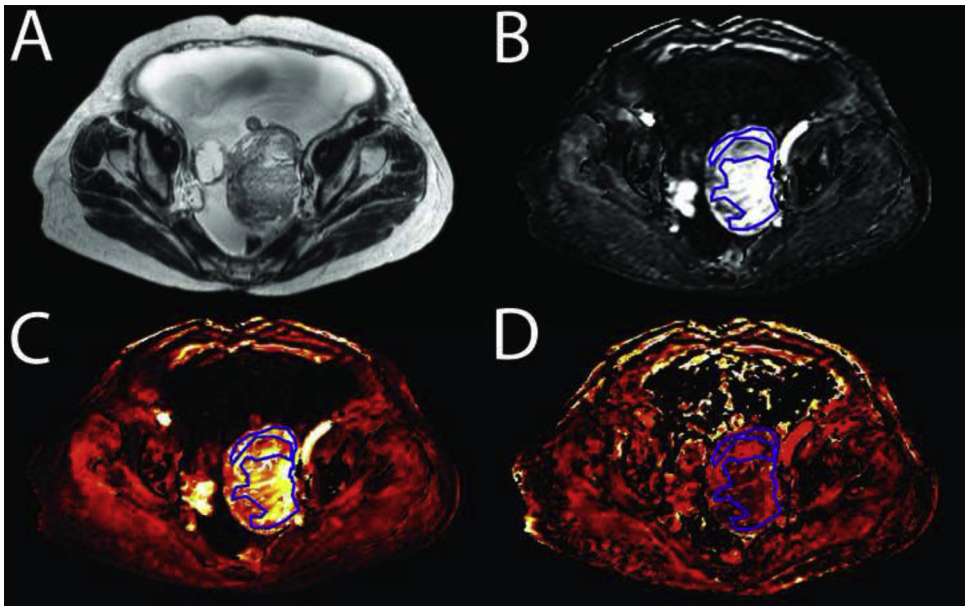

Fig. 2. Images from an 86-year-old woman with high grade (grade 3) serous ovarian adenocarcinoma. A primary tumor is seen in (A) T2-weighted, (B) enhanced images, and (C) with color-encoded K^{trans} (a rate constant for transfer of contrast agent from plasma to extravascular extracellular space (EES)) map, and (D) K_{ep} (a rate constant for transfer of contrast agent from EES to plasma) map.

Cox regression multivariate analysis. P ≤ 0.05 was considered significant, with high statistical significance set at P ≤ 0.01. Because of the exploratory nature of this study, we had decided to present p-values without the Bonferroni correction for multible comparisons.

3. Results

A total of 38 patients were recruited. Three patients were excluded from DCE imaging analyses because of insufficient image quality: one for different scanning time and two for movement artefacts. Thus, 35 patients with primary OC (mean age 67 years, range 47–86 years) were included. We also performed subgroup analyses with stage III and IV patients who did not receive NACT (n = 24). One patient did not undergo cytoreductive debulking surgery after neoadjuvant chemotherapy due to massive tumor burden, stage IV disease, large liver metastases that did not show response to chemotherapy, old age and poor performance status. Three other neoadjuvant patients had a good response to chemotherapy and they underwent debulking surgery. The mean largest solid tumor diameter in the plane where ROIs were placed was 75 mm (range 23–233 mm). Patients were followed up from the time of diagnosis until Septemper 2018.

Interobserver agreement was excellent for most of the DCE parameters (ICC, 0.951–0.994 for L-ROI; 0.928–0.991 for S-ROI) except for V_p and WashOut values, for which the two readers reached good agreement (Table 3). The Bland-Altman method was used to visualize interobserver reproducibility (Fig. 3). The Bland–Altman 95% limits of agreement were -1.83 – 2.09 for K^{trans} L-ROI and -1.70 – 2.22 for K^{trans} S-ROI, and coefficients of reproducibility were 0.27 and 0.53, respectively. Details of measurements for all DCE parameters (mean values) are shown in Supplementary Table 1.

Table 3
Interclass correlations (ICCs) between two readers from all the DCE parameters (mean values) used in analyses, both large regions of interest (L-ROIs) and small regions of interest (S-ROIs).

DCE parameter	ICC L-ROI	ICC S-ROI
K^{trans}	0.994	0.981
K_{ep}	0.990	0.952
V_e	0.997	0.965
V_p	0.637	0.614
AUC	0.991	0.991
Peak	0.971	0.944
Time to peak	0.975	0.790
WashIn	0.969	0.928
WashOut	0.951	0.584

AUC = area under the curve; ICC = Interclass correlation; L-ROI = large region of interest; S-ROI = small region of interest.

3.1. Association between DCE parameters and OC prognostic factors

Mean K^{trans} values were higher in high-grade serous OC than other types (L-ROI, 0.913 ± 0.952 vs. 0.425 ± 0.262, P = 0.041; S-ROI, 1.001 ± 1.051 vs. 0.436 ± 0.333, P = 0.018). FIGO stage, dichotomized into two separate groups (FIGO 1 + 2 versus FIGO 3 + 4) was associated positively with V_p minimum (S-ROI, 2.29 ± 1.84 vs. 5.89 ± 4.67, P = 0.023). An optimal cytoreductive result from the operation (R0 vs. residual tumor) was associated with higher mean K^{trans} (L-ROI, 0.874 ± 0.535 vs. 0.755 ± 1.140, P = 0.030; S-ROI, 0.967 ± 0.538 vs. 0.810 ± 1.330, P = 0.012; Fig. 4). Platinum sensitivity was associated with higher WashIn (maximum L-ROI, 3.23 ± 0.74 vs. 2.44 ± 0.80, P = 0.016; maximum S-ROI, 3.13 ± 0.81 vs. 2.39 ± 0.82, P = 0.031) and higher WashOut (mean L-ROI, 0.180 ± 0.090 vs. 0.111 ± 0.062, P = 0.034) levels. Other DCE parameters showed no statistically significant associations with traditional prognostic factors. In subgroup analysis higher K^{trans} remained significantly associated with high-grade serous OC (mean L-ROI, 1.08 ± 1.17 vs. 0.43 ± 0.30, P = 0.023; mean S-ROI, 1.21 ± 1.35 vs. 0.41 ± 0.33, P = 0.020) and with optimal cytoreductive result in staging surgery (mean L-ROI, 1.01 ± 0.43 vs. 0.78 ± 1.21, P = 0.020). Also higher V_e associated with high grade serous OC (mean S-ROI, 127.08 ± 119.82 vs. 40.17 ± 33.39, P = 0.010). Lower time-to-peak associated significantly (max S-ROI, 121.61 ± 124.09 vs. 186.04 ± 98.60, P = 0.030) with Platinum sensitivity. Supplementary tables 2 and 3 show the detailed results.

3.2. DCE MRI parameters vs. ADC values

ADC value was correlated with DCE parameter time-to-peak (mean L-ROI, r = 0.387, P = 0.026; maximum S-ROI, r = 0.366, P = 0.040), but not with other DCE parameters.

3.3. Recurrence free survival

In a median follow up of 57 months 15 of 35 patients experienced

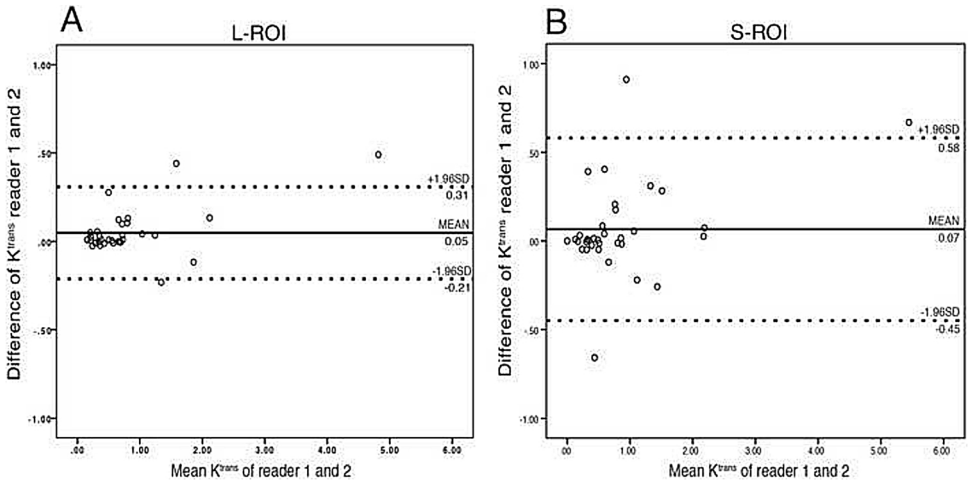

Fig. 3. Bland–Altman plots of K^{trans} measurements obtained by two readers using (A) large regions of interest (L-ROIs) and (B) small regions of interest (S-ROIs). The difference in K^{trans} values between the two readers (y-axis) is plotted against the mean K^{trans} of both readers (x-axis). The continuous line represents the mean absolute difference (bias) in K^{trans} between the two readers; the dashed lines represent the 95% confidence intervals of the mean difference (limits of agreement). The mean absolute difference in DCE K^{trans} measurements between the two readers is higher when S-ROI is used.

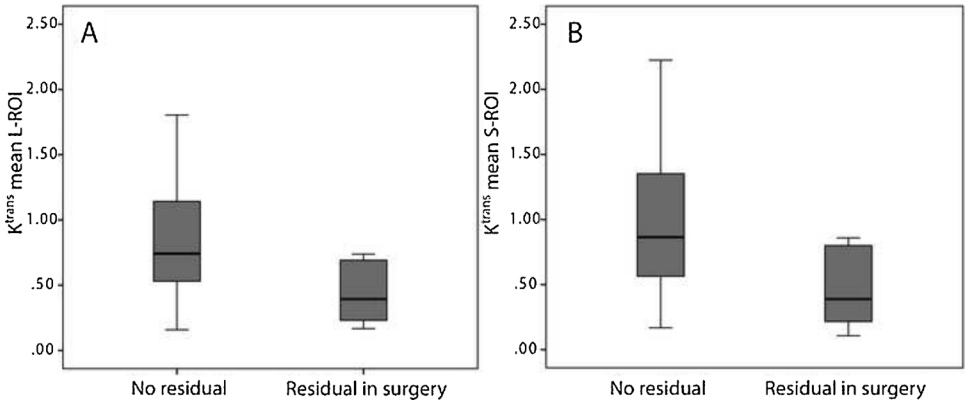

Fig. 4. The association between K^{trans} levels and surgery results. Optimal cytoreductive results with surgery (R0 or residual) were associated with higher mean K^{trans} (L-ROI, $P = 0.030$; S-ROI, $P = 0.012$).

recurrence. The median recurrence free survival (RFS) time was 19 months (range 6–68 months). In the univariate survival analysis DCE parameters lower time-to-peak (maximum S-ROI, P = 0.047), higher V_e (minimum L-ROI, P = 0.035; maximum S-ROI, P = 0.046) and higher V_p (maximum S-ROI, P = 0.033) correlated with shorter RFS in the Kaplan–Meier log-rank test (Fig. 5). Other significant predictors of shorter RFS were advanced stage (P = 0.011), presence of residual tumor at surgery (P = 0.008), non-sensitivity to platinum-based chemotherapy (P < 0.001), and partial response to treatment (P < 0.001).

We analysed survival data also for stage III and IV patients who did not receive NACT. In this 24 patient cohort V_p S-ROI minimum (P = 0.015), platinum resistance (P < 0.001) and progressive disease (P < 0.001) predicted shorter RFS.

To analyze whether multiparametric MRI (mpMRI) could even better predict the survival we made a combination variables of ADC and DCE parameters. Patients having both low ADC values and DCE parameters indicating more aggressive disease (higher in other DCE parameters but lower in time-to-peak) values were considered as 'poor prognostic mpMRI'. In the cohort of 35 patients the compination of low ADC and high V_e, V_p, WashIn, WashOut, Peak or low time-to-peak velue proved to be significant predictors for shorter RFS. When we used only stage III and IV patients without NACT (n = 24) the combination of low ADC and high V_e, V_p, WashOut and Peak velue remained significant predictors for shorter RFS, see Table 4. In a multivariate analysis using Cox regression none of the factors remained significant.

3.4. Overall survival

The median follow-up time was 38 months (range 2–90 months, two patients having died 2 months after diagnosis). At the end of follow-up, 14 (40%) patients with OC had died. None of the DCE parameters were associated with survival in Kaplan–Meier analysis. In univariate survival analysis, the presence of residual tumor (P < 0.001), incomplete response to treatment (P < 0.001), and poor response to platinum-based chemotherapy (P < 0.001) were significant predictors of poorer OS. Also the combination mpMRI variable with low ADC and high WashIn S-ROI minimum was significant (P = 0.033) (Table 4.). In the Cox multivariate regression analysis, only response to treatment (P = 0.001, complete response, hazard ratio (HR) 1; partial response P = 0.002, HR 57.833, confidential interval (CI) 4.650–719.286; progressive disease P < 0.001, HR 62.813, CI 6.792–580.899) proved to be an independent predictor of OS. We performed the survival analysis also with the subgroup of stage III and IV patients without NACT (n = 24). DCE parameter Time to Peak S-ROI maximum was significant (P = 0.037) in univariate survival analysis together with the same clinical parameters as in the cohort of 35 patients. None of the mpMRI combination parameters predicted survival. In the Cox multivariate regression analysis only response to treatment remained significant (P = 0.005, complete response, HR 1; P = 0.002, partial response HR 81.963 (CI 5.091–1319.485); P = 0.013 progressive disease HR 19.105 (CI 1.842–198.200)) although Time to Peak was nearly significant (P = 0.059, HR 3.556 (CI 0.954–13.253)).

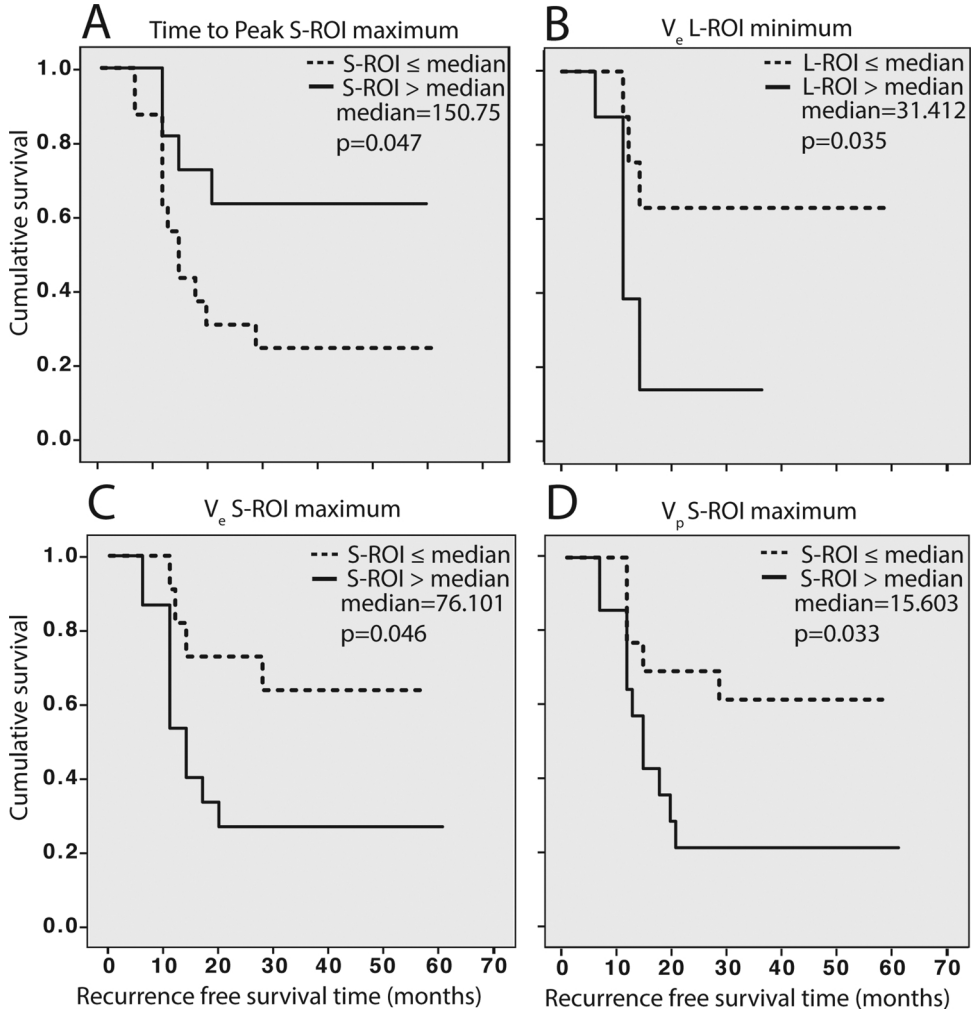

Fig. 5. In Kaplan–Meier survival analysis, (A) a lower time-to-peak (maximum small region of interest (S-ROI): $P = 0.047$), (B) higher V_e (minimum large region of interest (L-ROI): $P = 0.035$), (C) maximum S-ROI ($P = 0.046$), and (D) higher V_p (maximum S-ROI: $P = 0.033$) predict shorter recurrence-free survival (RFS).

Table 4
Univariate survival analysis ($p \leq 0.05$ considered significant) with multiparametric MRI variables. Multiparametric MRI parameter combined low ADC values (L-ROI < 0.821 mm^2/s and S-ROI < 0.688 mm^2/s) and DCE parameters indicating more aggressive disease (higher than median in other DCE parameters but lower than median in time-to-peak).

	RFS all 35 patients	RFS 24 patients	OS all 35 patients	OS 24 patients
V_e L-ROI min + low ADC	0.002	0.012	ns	ns
V_e S-ROI max + low ADC	0.002	0.020	ns	ns
V_e S-ROI min + low ADC	0.001	0.005	ns	ns
V_p L-ROI min + low ADC	< 0.001	0.005	ns	ns
V_p S-ROI mean + low ADC	0.009	ns	ns	ns
V_p S-ROI max + low ADC	0.005	ns	ns	ns
WashIn S-ROI min + low ADC	0.024	ns	0.033	ns
WashOut L-ROI mean + low ADC	ns	0.027	ns	ns
WashOut S-ROI min + low ADC	0.048	ns	ns	ns
Peak S-ROI mean + low ADC	0.001	0.005	ns	ns
Peak S-ROI max + low ADC	ns	0.012	ns	ns
Time-to-peak S-ROI mean + low ADC	0.050	ns	ns	ns
Time-to-peak S-ROI max + low ADC	0.007	ns	ns	ns

RFS = recurrence free survival, OS = overall survival, 24 patients were stage III and IV without neoadjuvant chemotherapy, S-ROI = Small ROI, L-ROI = large ROI, ns = not significant.

4. Discussion

It is important to characterize ovarian masses as precisely as possible before treatment. We prospectively enrolled 38 patients with OC to explore whether semi-quantitative and pharmacokinetic perfusion DCE parameters are associated with the clinical course of OC and could thus be used as prognostic imaging biomarkers. Our results suggest that several DCE parameters are linked to advanced OC and can predict earlier recurrence. Also in the subgroup analyses with only stage III and IV patients several of the DCE parameters remained as significant

prognostic factors.

Previous literature on correlations between DCE parameters and prognostic factors in other malignancies is promising. Many studies have shown that higher K^{trans}, K_{ep}, and V_e are associated with severity of disease [8,21,24], while others have not found as clear correlations between prognostic factors and DCE parameters [25,26]. In contrast, in cervical cancer, low K^{trans} was reported to be correlated with highly metastatic tumors [19]. The results of the present exploratory study suggest that values indicative of higher perfusion are associated to more aggressive OC.

In the present study, higher K^{trans} was associated with high-grade serous OC, shown to be the aggressive type of OC [27]. Residual tumor is one of the predictors of poor survival in OC [28]. Interestingly, K^{trans} correlated with the presence of residual tumor on surgery: the lower the K^{trans}, the bigger the risk for residual tumor in cytoreductive surgery. According to clinical experience, surgery is more likely to succeed if the tumor is highly vascular. With substantial fibrosis or a soft and fragile tumor, technical difficulties are more likely in surgery [29,30]. There are no earlier studies comparing K^{trans} values to cytoreductive surgical results.

Another important prognostic factor in OC is FIGO stage. Here, higher plasma volume fraction Vp correlated positively with FIGO stage, which is logical because tumors depend on angiogenesis and tumor neovascularization is strong in advanced stages [10,31]. Figo was dichotomized into FIGO 1 or 2 versus 3 or 4. Interestingly, in this cohort WashIn and WashOut parameters associated with platinum sensitivity, and WashOut remained significant also in the advanced stage subgroup. These findings need to be replicated in other cohorts. An imaging tool to estimate platinum sensitivity before treatment would be valuable.

Shorter recurrence free survival was predicted by higher V_e and V_p and lower time-to-peak in our cohort. Again, V_p reflects aggressive disease similar to low time-to-peak values. Earlier studies with perfusion parameters had discrepancies in predicting survival. Some studies found that a shorter enhanced time in the tumor predicted malignancy [6,11,13]. Other studies has showed that higher K^{trans} and K_{ep} corresponded with worse outcomes in breast cancer [24,32], while a study of cervical cancer showed that higher K^{trans} was associated with better RFS [20]. A previous OC study found no correlation with patient progression-free interval and DCE measurements [18].

We also created a multiparametric MRI variable combining low ADC and DCE parameters indicating more aggressive disease. In this analysis combinations of low ADC and high V_e, V_p, WashIn, WashOut, Peak or low time-to-peak parameters showed significant predictive value in the univariate survival analysis. Combinations of ADC and V_e, V_p, WashOut and Peak remained their signifigance also when the analysis was done only for the advanced stage subgroup (n = 24). Interestingly studies with multiparametric MRI in other cancers have shown that a combination of results from different sequencies seems to be superior compared to analyzing each of them separately [33,34]. Conflicting results between DCE parameters and prognostic factors in different studies may result partly from lack of consistent protocols for DCE studies and partly from differing patient cohorts and nature and behavior of tumors.

The ADC values did not show correlations to most of the DCE parameters suggesting that these parameters provide independent information on tumor biology. In general, lower ADC values are linked to high cellularity and solid tumors. Previous studies of DWI-MRI in OC support the view that lower ADC values are associated with more aggressive disease [5,35]. However, a weak positive correlation between time-to-peak and ADC values was found, giving support to an association of lower time-to-peak values with more aggressive disease. In OC, no earlier studies have investigated the possible correlation between ADC and time-to-peak. Sala et al. found a significant inverse correlation between pretreatment ADC and K_{ep} values [36].

Because of the known heterogenic nature of OC [37] and the exploratory nature of our study, we also registered minimum and maximum values inside the ROI in addition to mean values to study how the heterogeneous voxel distribution affects the results. For example for grading gliomas, maximal perfusion value proved to be the most accurate [38]. Some previous studies have used histogram analyses to demonstrate this heterogenic distribution[21,39]. Similar to our results, earlier studies indicate that not all measurements give significant results simultaneously; in the study by Kim et al., K^{trans}_{50} was associated with tumor size, but K^{trans}_{25} and K^{trans}_{75} yielded no significant associations [21].

A main limitation of this study is the small sample size. Because of the relatively small population, the number of different histological subtypes is small and larger cohorts are needed to confirm the results. Although patients with high grade serous histological type were most frequent in our cohort, their distribution to different FIGO stages was relatively similar to other histological types (Table 1). Another limitation is that we used a free-hand technique for ROI placement on single slices; while three-dimensional voxel-by-voxel analyses might have yielded more reliable results for biological tumor heterogeneity. Our software did not allow histogram analyses so we used mean, maximum and minimum values to estimate heterogeneity. B1 correction was not performed. The acquisition time was 6.7 s/stack in perfusion scan for 51 slices with an acquisition matrix of 269*387. AIF shape was inspected to be accurate for all patient individually. In further studies shorter temporal resolution may yield more robust data. When interpreting results from DCE-MRI studies, it should be noted that the selected acquisition strategy and analysis protocol affect the results, similar to type of contrast agent and data pre-processing. Only studies that use same type of scanners acquisition techniques and same analysis software are directly comparable.

A strength of our study is that we analyzed interobserver variability and obtained excellent ICC values for most DCE parameters and good ICC values for the remaining parameters. We aimed to explore the different DCE parameters and prognostic factors in OC as widely as possible. Therefore pharmacokinetic perfusion parameters and semi-quantitative measurements were included, although semi-quantitative values are not directly comparable.

In conclusion, semi-quantitatively measured and pharmacokinetic DCE perfusion parameters revealed associations with the clinical course and prognostic factors of patients with OC. As K^{trans} showed the highest associations with different prognostic factors and tumor aggressiveness, it may provide an imaging biomarker for future studies on OC. DCE parameters could also prove valuable in clinical practice and personalized medicine as K^{trans} could predict success of debulking surgery and WashIn and WashOut could predict response to platinum based chemotherapy. In diagnostic imaging protocol of OC a combination of tumor morphology, DWI and DCE parameters may be more useful than the single parameters. Further studies are needed to confirm our observations and clarify the prognostic value of DCE parameters in patients with OC.

Declaration of interest statement

None. Authors does not have any conflicts of interest.

Conflict of interest

The authors of this manuscript declare no relationships with any companies, whose products or services may be related to the subject matter of the article.

Funding

This study has received funding by Paavo Koistinen Foundation, Finnish adult education Foundation, Finnish Cultural Foundation, Kuopio University Hospital Research Foundation, Finnish Medical Foundation and Kuopio University Hospital (VTR grant).

Acknowledgments

We thank Antti Lindgren, Pauli Vainio and Tuomas Selander for their skillful technical assistance. This study was supported Paavo Koistinen Foundation, Finnish adult education Foundation, Finnish Cultural Foundation, Kuopio University Hospital Research Foundation, Finnish Medical Foundation and Kuopio University Hospital (VTR grant).

Appendix A. Supplementary data

Supplementary material related to this article can be found, in the online version, at doi:https://doi.org/10.1016/j.ejrad.2019.03.023.

References

[1] J.A. Ledermann, F.A. Raja, C. Fotopoulou, et al., ESMO Guidelines Working Group, newly diagnosed and relapsed epithelial ovarian carcinoma: ESMO Clinical Practice Guidelines for diagnosis, treatment and follow-up, Ann. Oncol. 24 (2013) 24–32, https://doi.org/10.1093/annonc/mdt333.

[2] J. Kaijser, T. Bourne, L. Valentin, et al., Improving strategies for diagnosing ovarian cancer: a summary of the International Ovarian Tumor Analysis (IOTA) studies, Ultrasound Obstet. Gynecol. 41 (2013) 9–20, https://doi.org/10.1002/uog.12323.

[3] S. Tingulstad, B. Hagen, F.E. Skjeldestad, et al., Evaluation of a risk of malignancy index based on serum CA125, ultrasound findings and menopausal status in the pre-operative diagnosis of pelvic masses, Br. J. Obstet. Gynaecol. 103 (1996) 826–831 http://www.ncbi.nlm.nih.gov/pubmed/8760716.

[4] K. Michielsen, R. Dresen, R. Vanslembrouck, et al., Diagnostic value of whole body diffusion-weighted MRI compared to computed tomography for pre-operative assessment of patients suspected for ovarian cancer, Eur. J. Cancer (2017), https://doi.org/10.1016/j.ejca.2017.06.010.

[5] A. Lindgren, M. Anttila, S. Rautiainen, et al., Primary and metastatic ovarian cancer: Characterization by 3.0T diffusion-weighted MRI, Eur. Radiol. 27 (2017) 4002–4012, https://doi.org/10.1007/s00330-017-4786-z.

[6] J. Ren, Y. Huan, H. Wang, et al., Dynamic contrast-enhanced MRI of benign prostatic hyperplasia and prostatic carcinoma: correlation with angiogenesis, Clin. Radiol. 63 (2008) 153–159, https://doi.org/10.1016/j.crad.2007.07.023.

[7] V.B. Ho, S.F. Allen, M.N. Hood, P.L. Choyke, Renal masses: quantitative assessment of enhancement with dynamic MR imaging, Radiology 224 (2002) 695–700, https://doi.org/10.1148/radiol.2243011048.

[8] H.R. Koo, N. Cho, I.C. Song, et al., Correlation of perfusion parameters on dynamic contrast-enhanced MRI with prognostic factors and subtypes of breast cancers, J. Magn. Reson. Imaging 36 (2012) 145–151, https://doi.org/10.1002/jmri.23635.

[9] P.S. Tofts, B. Berkowitz, M.D. Schnall, Quantitative analysis of dynamic Gd-DTPA enhancement in breast tumors using a permeability model, Magn. Reson. Med. 33 (1995) 564–568, https://doi.org/10.1002/mrm.1910330416.

[10] N. Paweletz, M. Knierim, Tumor-related angiogenesis, Crit. Rev. Oncol. Hematol. 9 (1989) 197–242, https://doi.org/10.1016/S1040-8428(89)80002-2.

[11] I. Thomassin-Naggara, M. Bazot, E. Daraï, et al., Epithelial ovarian tumors: value of dynamic contrast-enhanced MR imaging and correlation with tumor angiogenesis, Radiology 248 (2008) 148–159, https://doi.org/10.1148/radiol.2481071120.

[12] L. Bernardin, P. Dilks, S. Liyanage, et al., Effectiveness of semi-quantitative multiphase dynamic contrast-enhanced MRI as a predictor of malignancy in complex adnexal masses: radiological and pathological correlation, Eur. Radiol. 22 (2012) 880–890, https://doi.org/10.1007/s00330-011-2331-z.

[13] H.-M. Li, J.-W. Qiang, F.-H. Ma, S.-H. Zhao, The value of dynamic contrast-enhanced MRI in characterizing complex ovarian tumors, J. Ovarian Res. 10 (2017) 4, https://doi.org/10.1186/s13048-017-0302-y.

[14] I. Thomassin-Naggara, D. Balvay, E. Aubert, et al., Quantitative dynamic contrast-enhanced MR imaging analysis of complex adnexal masses: a preliminary study, Eur. Radiol. 22 (2012) 738–745, https://doi.org/10.1007/s00330-011-2329-6.

[15] R. Forstner, I. Thomassin-Naggara, T.M. Cunha, et al., ESUR recommendations for MR imaging of the sonographically indeterminate adnexal mass: an update, Eur. Radiol. 27 (2017) 2248–2257, https://doi.org/10.1007/s00330-016-4600-3.

[16] T. Taxt, R. Jirík, C.B. Rygh, et al., Single-channel blind estimation of arterial input function and tissue impulse response in DCE-MRI, IEEE Trans. Biomed. Eng. 59 (2012) 1012–1021, https://doi.org/10.1109/TBME.2011.2182195.

[17] S.P. Li, A. Makris, M.J. Beresford, et al., Use of Dynamic Contrast-enhanced MR Imaging to Predict Survival in Patients with Primary Breast Cancer Undergoing Neoadjuvant Chemotherapy, Radiology 260 (2011) 68–78, https://doi.org/10.1148/radiol.11102493.

[18] C.L. Mitchell, J.P.B. O'Connor, A. Jackson, et al., Identification of early predictive imaging biomarkers and their relationship to serological angiogenic markers in patients with ovarian cancer with residual disease following cytotoxic therapy, Ann. Oncol. 21 (2010) 1982–1989, https://doi.org/10.1093/annonc/mdq079.

[19] K.M. Øvrebø, C. Ellingsen, T. Hompland, E.K. Rofstad, Dynamic contrast-enhanced magnetic resonance imaging of the metastatic potential of tumors: a preclinical study of cervical carcinoma and melanoma xenografts, Acta Oncol. (Madr). 52 (2013) 604–611, https://doi.org/10.3109/0284186X.2012.689851.

[20] B.R. Dickie, C.J. Rose, L.E. Kershaw, et al., West, the prognostic value of dynamic contrast-enhanced MRI contrast agent transfer constant K(trans) in cervical cancer is explained by plasma flow rather than vessel permeability, Br. J. Cancer 116 (2017) 1436–1443, https://doi.org/10.1038/bjc.2017.121.

[21] S.H. Kim, H.S. Lee, B.J. Kang, et al., Dynamic contrast-enhanced MRI perfusion parameters as imaging biomarkers of angiogenesis, PLoS One 11 (2016) e0168632, , https://doi.org/10.1371/journal.pone.0168632.

[22] C.A. Cuenod, D. Balvay, Perfusion and vascular permeability: basic concepts and measurement in DCE-CT and DCE-MRI, Diagn. Interv. Imaging 94 (2013) 1187–1204, https://doi.org/10.1016/j.diii.2013.10.010.

[23] H. Bickel, K. Pinker, S. Polanec, et al., Diffusion-weighted imaging of breast lesions: region-of-interest placement and different ADC parameters influence apparent diffusion coefficient values, Eur. Radiol. (2017), https://doi.org/10.1007/s00330-016-4564-3.

[24] F. Liu, M. Wang, H. Li, Role of perfusion parameters on DCE-MRI and ADC values on DWMRI for invasive ductal carcinoma at 3.0 Tesla, World J. Surg. Oncol. (2018), https://doi.org/10.1186/s12957-018-1538-8.

[25] H. Wright, J. Listinsky, C. Quinn, Increased ipsilateral whole breast vascularity as measured by contrast-enhanced magnetic resonance imaging in patients with breast cancer, in: Am. J. Surg. (2005), https://doi.org/10.1016/j.amjsurg.2005.06.015.

[26] P. Andrzejewski, G. Wengert, T.H. Helbich, et al., Sequential [18F]FDG-[18F] FMISO PET and multiparametric MRI at 3T for insights into breast Cancer heterogeneity and correlation with patient outcomes: first clinical experience, Contrast Media Mol. Imaging (2019), https://doi.org/10.1155/2019/1307247.

[27] C.B. Gilks, D.N. Ionescu, S.E. Kalloger, et al., Tumor cell type can be reproducibly diagnosed and is of independent prognostic significance in patients with maximally debulked ovarian carcinoma, Hum. Pathol. 39 (2008) 1239–1251, https://doi.org/10.1016/j.humpath.2008.01.003.

[28] A. du Bois, A. Reuss, E. Pujade-Lauraine, et al., Role of surgical outcome as prognostic factor in advanced epithelial ovarian cancer: a combined exploratory analysis of 3 prospectively randomized phase 3 multicenter trials, Cancer 115 (2009) 1234–1244, https://doi.org/10.1002/cncr.24149.

[29] R.K. Wong, V. Tandan, S. De Silva, A. Figueredo, Pre-operative radiotherapy and curative surgery for the management of localized rectal carcinoma, in: cochrane, Database Syst. Rev. (2007), https://doi.org/10.1002/14651858.CD002102.pub2.

[30] K. Sato, S. Ito, T. Kitagawa, et al., Factors affecting the technical difficulty and clinical outcome of endoscopic submucosal dissection for colorectal tumors, Surg. Endosc. 28 (2014) 2959–2965, https://doi.org/10.1007/s00464-014-3558-y.

[31] H.C. Hollingsworth, E.C. Kohn, S.M. Steinberg, et al., Tumor angiogenesis in advanced stage ovarian carcinoma, Am. J. Pathol. 147 (1995) 33–41 http://www.ncbi.nlm.nih.gov/pubmed/7541612.

[32] S.P. Li, A. Makris, M.J. Beresford, et al., Use of dynamic contrast-enhanced MR imaging to predict survival in patients with primary breast cancer undergoing neoadjuvant chemotherapy, Radiology 260 (2011) 68–78, https://doi.org/10.1148/radiol.11102493.

[33] J.J. Park, C.K. Kim, S.Y. Park, et al., Prostate cancer: role of pretreatment multiparametric 3-T MRI in predicting biochemical recurrence after radical prostatectomy, Am. J. Roentgenol (2014), https://doi.org/10.2214/AJR.13.11381.

[34] K. Pinker, L. Moy, E.J. Sutton, et al., Diffusion-weighted imaging with apparent diffusion coefficient mapping for breast Cancer detection as a stand-alone parameter: comparison with dynamic contrast-enhanced and multiparametric magnetic resonance imaging, Invest. Radiol. (2018), https://doi.org/10.1097/RLI.0000000000000465.

[35] J.-W. Oh, S.E. Rha, S.N. Oh, et al., Diffusion-weighted MRI of epithelial ovarian cancers: correlation of apparent diffusion coefficient values with histologic grade and surgical stage, Eur. J. Radiol. 84 (2015) 590–595, https://doi.org/10.1016/j.ejrad.2015.01.005.

[36] E. Sala, M.Y. Kataoka, a.N. Priest, et al., Advanced ovarian Cancer: multiparametric MR imaging demonstrates response- and metastasis-specific effects, Radiology 263 (2012) 149–159, https://doi.org/10.1148/radiol.11110175.

[37] H.A. Vargas, H. Veeraraghavan, M. Micco, et al., A novel representation of inter-site tumour heterogeneity from pre-treatment computed tomography textures classifies ovarian cancers by clinical outcome, Eur. Radiol. 27 (2017) 3991–4001, https://doi.org/10.1007/s00330-017-4779-y.

[38] A. Hilario, A. Ramos, A. Perez-Nuñez, et al., The added value of apparent diffusion coefficient to cerebral blood volume in the preoperative grading of diffuse gliomas, AJNR Am. J. Neuroradiol. 33 (2012) 701–707, https://doi.org/10.3174/ajnr.A2846.

[39] F. Davnall, C.S.P. Yip, G. Ljungqvist, et al., Assessment of tumor heterogeneity: an emerging imaging tool for clinical practice? Insights Imaging 3 (2012) 573–589, https://doi.org/10.1007/s13244-012-0196-6.